Journal of Statistical Physics, Vol. 51, Nos. 3/4, 1988

Distribution Functions for Fluids in Random Media

William G. Madden[1] **and Eduardo D. Glandt**[2]

Received October 27, 1988

A random medium is considered, composed of identifiable interactive sites or obstacles equilibrated at a high temperature and then quenched rapidly to form a rigid structure, statistically homogeneous on all but molecular length scales. The equilibrium statistical mechanics of a fluid contained inside this quenched medium is discussed. Various particle–particle and particle–obstacle correlation functions, which differ from the corresponding functions for a fully equilibrated binary mixture, are defined through an averaging process over the static ensemble of obstacle configurations and application of topological reduction techniques. The Ornstein–Zernike equations also differ from their equilibrium counterparts.

KEY WORDS: Random media; correlation functions; graph theory; inhomogeneous fluids; random fields.

1. INTRODUCTION

There are many situations in which a fluid, either a liquid or a vapor, is introduced into a random structure that is statistically homogeneous on all but molecular length scales. The response of the medium to the presence of the fluid phase can vary substantially: it may dissolve into the fluid, it may swell or contract considerably, or there may be virtually no structural response. In this last limit, the rigid structure can be regarded as a random field of obstacles within which the fluid establishes itself in a state of thermodynamic equilibrium.

The statistical mechanics for fluids in external fields is well established, and is often used to produce relationships among the distribution functions

---

[1] Polymer Products Department, E. I. Du Pont de Nemours & Company, Experimental Station, Wilmington, Delaware 19898.

[2] Department of Chemical Engineering, University of Pennsylvania, Philadelphia, Pennsylvania 19104.

0022-4715/88/0500-0537$06.00/0 © 1988 Plenum Publishing Corporation

of a field-free fluid by introducing additional particles as external fields.(1–4) In the present application, however, the field acting on each fluid particle is defined by the local structure of the rigid obstacles and varies irregularly throughout the macroscopic sample. The formal development for particles in external fields leads to equations that combine the complexity of the fluid with that of the field. Even when the potential energy can be represented by pairwise interactions of the fluid particles with one another and with specific "sites" in the medium, it is not immediately clear how the distributions of fixed sites can be incorporated into the problem in a simple fashion.

For a fluid in a rigid, random medium, the symmetry of the system and/or its Hamiltonian is clearly similar to that of a two-component mixture in complete thermodynamic equilibrium. Our goal is to exploit this similarity to cast the problem at hand in an analogous form. In the most general case, the obstacles can be characterized completely only in terms of a hierarchy of distribution functions. However, this immobile phase will often have been produced by a quench from some higher temperature at which a state of true thermodynamic equilibrium existed. If no major structural relaxation of the immobile phase occurred during the quench, the resulting structure may be approximated by that at the higher temperature. This allows us to use conventional techniques of topological reduction to recast the problem into a mixturelike form. However, this quenched equilibrium limit must be embedded in a more general theory, which we will derive elsewhere via a different route.

In contrast to the earlier work by Frisch(5) and Torquato and Stell,(6–10) we focus attention on distribution functions that correspond to interaction sites on the molecules that make up the obstacles and the fluid. The "matrix functions" introduced by Frisch probe the shape of the volume occluded by a rigid, impenetrable boundary. Our analysis, based on familiar graph theory, does not require that there be so absolute a division between the rigid and mobile phases. The hierarchy of matrix functions is of great interest, in part because it also serves to describe the structure of media that are heterogeneous at much larger length scales. Torquato and Stell(6) were able to represent these functions as an unusual kind of graphical series. The rigidity of the matrix enters both graphical analyses in a similar way, and we believe that much of what we present here will prove useful in the Torquato–Stell approach as well.

2. EQUILIBRIUM IN A RIGID MEDIUM

Consider a very large sample of the fixed medium (*m*), not necessarily at thermodynamic equilibrium, made up of immobile sites or "obstacles."

This system may be divided into a large number of macroscopic subsamples (or "realizations"), each of volume V, which are in mutual thermal and mechanical equilibrium. In a particular realization there will be M obstacles located at positions $\{\mathbf{q}_1, \mathbf{q}_2, \ldots, \mathbf{q}_M\} = \mathbf{q}^M$. The subset of all realizations containing precisely M obstacles in found with probability P_M and, within that subset, the obstacles are distributed with probability density $P^{(M)}(\mathbf{q}^M)$.

A fluid (f) of mobile "particles" is introduced into the medium and allowed to come to equilibrium with some specified activity z_f and reciprocal temperature $\beta = (kT)^{-1}$. At any instant, a typical realization of the medium will contain N particles located at $\mathbf{r}_1, \mathbf{r}_2, \ldots, \mathbf{r}_N$. As the system evolves, the particles will be distributed according to a grand canonical ensemble. Because the obstacle field varies from one realization to another, each fluid sample will access a distinct equilibrium ensemble. For a specified realization, the conditional probability density for the mobile phase is

$$P(\mathbf{r}^N \mid \mathbf{q}^M) = [\Xi_f(\mathbf{q}^M)]^{-1} z_f^N \exp[-\beta U_{NM}(\mathbf{r}^N; \mathbf{q}^M)] \tag{1}$$

where U_{NM} is the potential energy of the N particles in the presence of the M obstacles, and where $\Xi_f(\mathbf{q}^M)$ is the field-dependent grand partition function

$$\Xi_f(\mathbf{q}^M) = \sum_N \frac{z_f^N}{N!} \int d\mathbf{r}^N \exp[-\beta U_{NM}(\mathbf{r}^N; \mathbf{q}^M)] \tag{2}$$

For a specified obstacle realization ($\mathbf{q}^M$), the average of any mechanical variable $X(\mathbf{r}^N; \mathbf{q}^M)$ is

$$\begin{aligned}\langle X \rangle_f &= \sum_N \frac{1}{N!} \int d\mathbf{r}^N X(\mathbf{r}^N; \mathbf{q}^M) P(\mathbf{r}^N \mid \mathbf{q}^M) \\ &= [\Xi_f(\mathbf{q}^M)]^{-1} \sum_N \frac{z_f^N}{N!} \int d\mathbf{r}^N X(\mathbf{r}^N; \mathbf{q}^M) \exp[-\beta U_{NM}(\mathbf{r}^N; \mathbf{q}^M)] \end{aligned} \tag{3}$$

where $\langle \cdots \rangle_f$ is used to indicate that the average is taken over the fluid ensemble only, so that the resulting quantity is a function of $\mathbf{q}^M$. Any such quantity $Y(\mathbf{q}^M)$ may be further averaged over the static ensemble of obstacles

$$\langle Y \rangle_m = \sum_M \frac{P_M}{M!} \int d\mathbf{q}^M \, Y(\mathbf{q}^M) \, P^{(M)}(\mathbf{q}^M) \tag{4}$$

where $\langle \cdots \rangle_m$ indicates this second type of average. The $Y(\mathbf{q}^M)$ need not be the partially averaged mechanical variables defined by Eq. (3). The extensive nature of the "supersystem" used in the construction of the ensemble for the obstacles also allows the direct averaging of non-mechanical quantities such as entropy and free energy over the distribution of obstacles.

To facilitate further analysis, we now identify the distribution of obstacles with an equilibrium distribution originally established at some different inverse temperature β_m

$$P_M P^{(M)}(\mathbf{q}^M) = [\Xi_m]^{-1} z_m^M \exp[-\beta_m W_M(\mathbf{q}^M)] \tag{5}$$

where z_m is the activity of the pure matrix sites prior to quenching, $W_M(\mathbf{q}^M)$ is the potential energy of an obstacle configuration, and Ξ_m is the grand canonical partition function for the prequench medium. Substitution of Eqs. (3) and (5) into Eq. (4) gives, for the average of any mechanical quantity $X(\mathbf{r}^N; \mathbf{q}^M)$,

$$\begin{aligned}\langle X \rangle = [\Xi_m]^{-1} \sum_M \sum_N z_m^M z_f^N (M!\, N!)^{-1} \\ \times \int d\mathbf{q}^M \, [\Xi_f(\mathbf{q}^M)]^{-1} \, d\mathbf{r}^N \, X(\mathbf{r}^N; \mathbf{q}^M) \\ \times \exp[-\beta U_{NM}(\mathbf{r}^N; \mathbf{q}^M) - \beta_m W_M(\mathbf{q}^M)]\end{aligned} \tag{6}$$

When no subscript is attached to the angled brackets, they indicate that a mechanical quantity has been averaged first over the fluid ensemble and then over the ensemble of obstacle configurations. Equation (6) may be compared with the corresponding expression for a mixture in complete thermodynamic equilibrium and characterized by a single temperature β

$$\begin{aligned}\langle X \rangle_{\text{mix}} = [\Xi]^{-1} \sum_M \sum_N z_m^M z_f^N (M!\, N!)^{-1} \\ \times \int d\mathbf{q}^M \, d\mathbf{r}^N \, X(\mathbf{r}^N; \mathbf{q}^M) \exp\{-\beta[U_{NM}(\mathbf{r}^N; \mathbf{q}^M) + W_M(\mathbf{q}^M)]\}\end{aligned} \tag{7}$$

The presence of two different temperatures in Eq. (6), while of quantitative significance, does not affect the mathematical structure of the integral and has no formal effect on any subsequent analysis. The irreconcilable difference between Eqs. (6) and (7) arises from the presence in the former of the partition function $\Xi_f(\mathbf{q}^M)$ within the integral over obstacle positions.

If the interactions are pairwise additive, the expressions for the most important mechanical averages can be written in terms of the appropriate singlet and pair densities $\rho^{(1)}(\mathbf{r}_1)$ and $\rho^{(2)}(\mathbf{r}_1, \mathbf{r}_2)$. For both the medium (frozen in a near-equilibrium configuration) and the fluid (in contact with a specific realization of the medium and in true equilibrium) these are given by the usual *pure fluid* expressions

$$\rho_m^{(n)}(\mathbf{q}_1,\ldots,\mathbf{q}_n)=[\Xi_m]^{-1}\sum_{M\geqslant n}\frac{z_m^M}{(M-n)!}\times\int d\mathbf{q}_{n+1}\cdots d\mathbf{q}_M\exp[-\beta_m W_M(\mathbf{q}^M)] \tag{8}$$

and

$$\hat{\rho}_f^{(n)}(\mathbf{r}_1,\ldots,\mathbf{r}_n;\mathbf{q}^M)=[\Xi_f(\mathbf{q}^M)]^{-1}\sum_{N\geqslant n}\frac{z_f^N}{(N-n)!}\times\int d\mathbf{r}_{n+1}\cdots d\mathbf{r}_N\exp[-\beta U_{NM}(\mathbf{r}^N;\mathbf{q}^M)] \tag{9}$$

The caret that has been added to $\rho_f^{(n)}$ and that will be used on other fluid quantities emphasizes that these definitions apply to a specific realization $(\mathbf{q}^M)$ of the matrix.

The important theoretical and experimental quantities are the averages of the $\hat{\rho}_f^{(n)}(\mathbf{r}_1,\ldots,\mathbf{r}_n;\mathbf{q}^M)$ over all configurations of the obstacles

$$\rho_f^{(n)}(\mathbf{r}_1,\ldots,\mathbf{r}_n)=\sum_M\frac{P_M}{M!}\int d\mathbf{q}^M\,P^{(M)}(\mathbf{q}^M)\,\hat{\rho}_f^{(n)}(\mathbf{r}_1,\ldots,\mathbf{r}_n;\mathbf{q}^M) \tag{10}$$

To simplify the presentation, but without a significant loss of generality, we assume that both U_{NM} and W_M are pairwise additive

$$U_{NM}(\mathbf{r}^N;\mathbf{q}^M)=\sum_{i<j}^{N}u(\mathbf{r}_i,\mathbf{r}_j)+\sum_i^N\sum_k^M v(\mathbf{r}_i,\mathbf{q}_k) \tag{11}$$

and

$$W_M(\mathbf{q}^M)=\sum_{k<l}^{M}w(\mathbf{q}_k,\mathbf{q}_l) \tag{12}$$

where u, v, and w are the particle–particle, particle–obstacle, and obstacle–obstacle pair potentials, respectively. Upon exponentiation, the sums of potentials become products of exponentials, which may then be expressed in terms of the Mayer f-functions $f_u\equiv e^{-\beta u}-1$, $f_v\equiv e^{-\beta v}-1$, and $f_w\equiv e^{-\beta_m w}-1$. The probability densities and partition functions can then be expanded, and the resulting integrals can be represented graphically in a form suitable for topological reduction.

The process of topological reduction has been well described[1-3,11,12] and will only be summarized here to make clear how the present analysis differs from that for an equilibrium mixture. An arbitrary external field (which vanishes under homogeneous bulk conditions) is usually introduced for convenience. In the case of a pure fluid, the integrals in the infinite series can be represented by graphs whose bonds are f-bonds, whose field points denote integrals over $d\mathbf{r}_i$, and whose labeled root points represent a functional dependence on the variable indicated by the label. All points are weighted by a local activity $z(\mathbf{r}_i)$, which includes in its definition the exponential of any singlet external potentials. Symmetry numbers are included in the definition of the graphs to account for multiple occurrences of identical terms. The reciprocal of the partition function remains as a prefactor for the entire graphical series of the distribution functions.[1]

The graphs contributing to the distribution functions are not necessarily connected, and in such cases represent factorable integrals. The disconnected fragments containing no root points are recognized as graphs in the expansion of the partition function. Their sum, which can be factored out of all unique rooted structures, cancels the factor Ξ^{-1}. The graphical representations of the distribution functions become sums of graphs having at least one path of bonds connecting each field point to at least one root. Of course, this graphical representation is reached more quickly by successive functional differentiation of the graphical series for $\ln \Xi$ with respect to the generalized activities.[2] The present case, however, lacks a joint partition function to represent implicitly the entire structure of the fluid–obstacle system.

For the analysis that follows it is necessary to make careful distinctions among the various activities and number densities that characterize the fluid. By construction, there is a single activity z_f identical for all realization-dependent fluid ensembles. If an arbitrary external field $\psi(\mathbf{r}_i)$ were applied identically to each realization of the obstacles, the local activity would be defined by $z_f^*(\mathbf{r}_i) = z_f \exp[-\beta\psi(\mathbf{r}_i)]$. This is the field that is allowed to vanish under homogeneous bulk conditions. In the present application there is an additional permanent external field, representing the interactions of the fluid with the obstacles,

$$\phi(\mathbf{r}_i; \mathbf{q}^M) = \exp\left[-\sum_k \beta v(\mathbf{r}_i, \mathbf{q}_k)\right] = \prod_k [f_v(\mathbf{r}_i, \mathbf{q}_k) + 1] \tag{13}$$

which leads to a realization-dependent local activity $\hat{z}_f^*(\mathbf{r}_i; \mathbf{q}^M) = z_f^*(\mathbf{r}_i)\, \phi(\mathbf{r}_i; \mathbf{q}^M)$.

In the presence of both the obstacle field and any other arbitrary field ψ, an important quantity is the singlet density $\hat{\rho}_f^{(1)}(\mathbf{r}_i; \mathbf{q}^M)$, given by Eq. (9)

with $n=1$. Averaging $\hat{\rho}_f^{(1)}(\mathbf{r}_i; \mathbf{q}^M)$ over the system volume V yields the mean fluid density within that realization,

$$\hat{\rho}_f(\mathbf{q}^M) = V^{-1} \int d\mathbf{r}_i \, \hat{\rho}_f^{(1)}(\mathbf{r}_i; \mathbf{q}^M) \tag{14}$$

In general, each realization will have a different mean fluid density at equilibrium. The global mean fluid density, averaged over the ensemble of obstacle configurations, is

$$\rho_f = V^{-1} \int d\mathbf{r}_i \, \rho_f^{(1)}(\mathbf{r}_i) = \langle \hat{\rho}_f(\mathbf{q}^M) \rangle_M \tag{15}$$

One of our goals is to obtain graphical expressions that eliminate the various activities in favor of the averaged quantities $\rho_f^{(1)}(\mathbf{r}_i)$, $\rho_m^{(1)}(\mathbf{q}_i)$, ρ_f, and ρ_m.

In the activity expansions of $\hat{\rho}_f^{(1)}(\mathbf{r}_1; \mathbf{q}^M)$ and $\hat{\rho}_{ff}^{(2)}(\mathbf{r}_1, \mathbf{r}_2; \mathbf{q}^M)$, all the graphs are connected; they contain articulation circles, and the points represent the activity $\hat{z}_f^*(\mathbf{r}_i; \mathbf{q}^M)$. Let $\Gamma(\mathbf{r}_1; \mathbf{q}^M)$, an arbitrary graph (or its associated function) appearing in the expansion of $\hat{\rho}_f^{(1)}$, be inserted into Eq. (10). Both $\exp[-\beta W(\mathbf{q}^M)]$ and $\phi(\mathbf{r}_i; \mathbf{q}^M)$ can be expanded in f_v and f_w functions, and the integration over $\mathbf{q}^M$ performed. From the single graph $\Gamma(\mathbf{r}_1; \mathbf{q}^M)$, an infinite series of integrals is generated, which can be represented by graphs with varying numbers of f_u, f_v, and f_w bonds connecting the points of the original graph to any number of obstacle field points, each associated with an activity $z_m^*(\mathbf{q}_i)$. The field points are now associated with the mean local activity $z_f^*(\mathbf{r}_i)$. The structure of the obstacles is represented implicitly by the presence of f_w bonds and the attendant large increase in the number of graphs. Many of the topologically distinct graphs representing terms in this series are now disconnected, but all disconnected fragments are made up entirely of obstacle field points and f_w bonds. The set of topologically unique graphs arising from a particular graph $\Gamma(\mathbf{r}_1; \mathbf{q}^M)$ is completely disjoint from that arising from any other distinguishable graph $\Gamma'(\mathbf{r}_1; \mathbf{q}^M)$.

By analogy with the description of the general procedure, the integrals are expressed as products, and the corresponding graphs are separated into a singly rooted fragment and unrooted, disconnected subgraphs. The sum of all graphs with the same core is equal to the product of the rooted fragment times the partition function Ξ_m. This cancels the reciprocal of the partition function, which normalizes the distribution of obstacles. The resulting series is the sum of all such connected graphs, similar to (but smaller than) the set that would be obtained for a true equilibrium mixture. To identify the missing graphs, we define an *articulation set* as a set of points whose removal would disconnect a graph into two or more fragments, at least one of which contains only field points. An obstacle articulation set is one made up entirely of obstacle points, and a *shielding set* is an obstacle articulation set whose removal produces unrooted, disjoint fragments containing at least one fluid field point. *All graphs with shielding sets are absent* from the expression for the distribution functions of the fluid in the averaged medium. This is physically appealing because, by postulate, the matrix is rigid and the obstacles do not respond to the forces generated by the mobile particles. While individual graphs should not be given a physical interpretation that is too literal, the sets do represent the interactions of particles on one "side" with those on the other "side" of the set through the redistribution of the obstacles themselves. It is thus reasonable that such graphs be excluded.

It is interesting to consider how those particular graphs, present in a true equilibrium mixture, came to be absent here. In both the equilibrium mixture and the problem at hand, expansion of the potential energies into products of f-bonds generates an identical number of terms prior to any integrations. In the true equilibrium mixture there is a unique distribution function that normalizes each of the singlet and mixed pair distribution functions. The cancellation of disconnected graphs occurs only after all integrations over the positions of both components are performed. The conditional probability formulation of the present problem leads to two distinct probability distributions. *Whether or not the obstacle probability function is of the equilibrium form assumed here*, there is a unique fluid partition function $\Xi_f(\mathbf{q}^M)$ for each obstacle configuration. There is therefore always a complete removal of disconnected graphs in the fluid distribution functions, which is separate for each realization of the fixed matrix. Thus, those integrands that would have been connected upon integration over the second component are removed in the cancellation of $\Xi_f(\mathbf{q}^M)$.

This process is illustrated in Fig. 1, where squares and circles are used to indicate obstacle and fluid points, respectively. The graph on the left represents a partially integrated term contributing to a singlet distribution function. In the equilibrium mixture, the completion of the remaining integrations leads to the graph at the top. In the random medium problem, however, the top part of the graph, shown in brackets, is merely one contribution to one of the disconnected graphs. The parent graph is shown, with asterisks used to indicate field points in the full M-obstacle external potential. This rootless portion of the parent graph contributes to the cancellation of $\Xi_f(\mathbf{q}^M)$, and only the connected residual, free of shielding pairs, survives in the final formulation of the graphical series, given below:

$\rho_f^{(1)}(\mathbf{r}_1)$ = sum of all topologically distinct, simple, connected graphs with one fluid root point (representing the factor z_f^*), some or no fluid field points (representing the factor z_f^*), some or no obstacle field points (representing the factor z_m^*), some or no f_u bonds between pairs of fluid points, some or no f_v bonds between mixed pairs of points, and some or no f_w bonds between pairs of obstacle points, such that the graphs have no shielding sets (16)

Exactly the same kind of analysis can be carried out for $\rho_f^{(n)}(\mathbf{r}_1,..., \mathbf{r}_n)$, except that the graphical series contains n fluid root points. (When a single subscript is used for a higher order function, all root points are of the same species.) The graphical expressions for the pair and higher distribution functions can be further simplified. For this purpose it is useful to define general n-body correlation functions $g^{(n)}$ as the ratio of the $\rho^{(n)}$ to their ideal-gas limits,

$$g^{(n)}_{\alpha,...,\nu}(\mathbf{x}_1,..., \mathbf{x}_n) = \frac{\rho^{(n)}_{\alpha,...,\nu}(\mathbf{x}_1,..., \mathbf{x}_n)}{\rho_\alpha^{(1)}(\mathbf{x}_1) \cdots \rho_\nu^{(1)}(\mathbf{x}_n)} \tag{17}$$

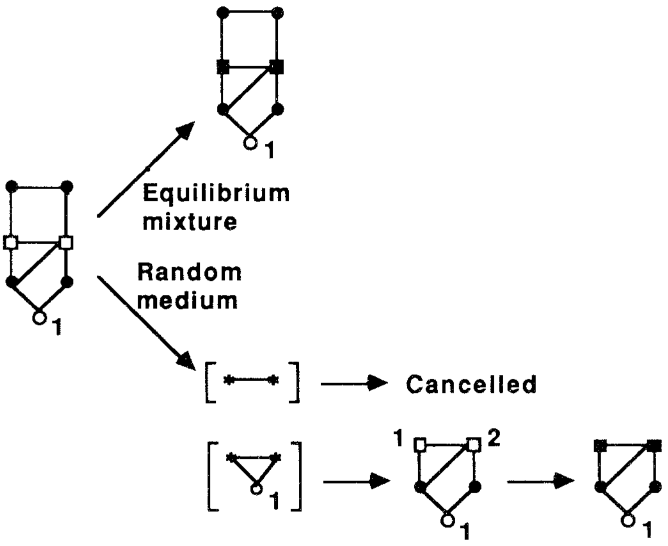

Fig. 1. Graphical expansions of the singlet distribution function for an equilibrium binary mixture and for a fluid in a quenched medium. The circles and squares rpresent fluid and obstacle particles, respectively. The resulting diagrams in the random medium case are free of shielding sets. The graph formed by the two disconnected fluid particles is cancelled by the partition function $\Xi_f(\mathbf{q}^M)$.

The subscripts indicate the species involved (m or f), and $\mathbf{x}$ denotes $\mathbf{q}$ or $\mathbf{r}$, as appropriate.

In any graph contributing to the $\rho_f^{(n)}$, there is a minimal set of articulation points (including the roots themselves), one of which lies on every path from one of the remaining articulation points to any root. When this minimal set is removed, the unrooted fragments result in residuals that are elements of the graphical expansion of one of the singlet densities. The obstacle articulation points, upon removal, produce disconnected, unrooted fragments with only obstacle points. (Otherwise, they would be shielding 1-sets.) Those disconnected fragments are members of the graphical series for $\rho_m^{(1)}(\mathbf{r})$, which has the usual topological specification for a pure fluid. The topological reduction can then be carried out to remove residuals articulated at obstacle points by replacing them with $\rho_m^{(1)}(\mathbf{r})$ points. The fragments eliminated at fluid articulation points are all graphical elements of the series described in Eq. (16). Appropriate reduction at these points replaces the fragments by $\rho_f^{(1)}(\mathbf{r})$ field points, so that only graphs without articulation points remain. The definition of the $g_f^{(n)}$ gives a graphical series which has unit weighting at the roots and is (at this level of specification) otherwise identical to that for $\rho_f^{(n)}$. Both are identical to those that would arise in an equilibrium mixture, except that graphs with shielding sets are absent here.

The structure of the fluid in the neighborhood of an obstacle is also of interest. At lowest order, this structure is represented by the mixed pair density functions, related by symmetry.

$$\rho_{fm}^{(2)}(\mathbf{r}_1, \mathbf{q}_1) = \rho_{mf}^{(2)}(\mathbf{q}_1, \mathbf{r}_1) \tag{18}$$

For a specific realization of the matrix, setting $n = 1$ in Eq. (9) gives the singlet density $\hat{\rho}_f^{(1)}(\mathbf{r}_1; \mathbf{q}^M)$. For a quenched distribution of M obstacles, the probability density that there is a fluid particle at position $\mathbf{r}_1$ conditional on the presence of *any* obstacle at $\mathbf{q}_1$ is

$$\tilde{\rho}_{f|m}^{(1)}(\mathbf{r}_1 | \mathbf{q}_1) = \frac{M!}{(M-1)!} \int d\mathbf{q}_1 \cdots d\mathbf{q}_M \frac{\exp[-\beta_m W_M(\mathbf{q}^M)]}{Z_m} \hat{\rho}_f^{(1)}(\mathbf{r}_1; \mathbf{q}^M) \tag{19}$$

where $Z_m = \int d\mathbf{q}^M \exp[-\beta_m W_M(\mathbf{q}^M)]$ is the configurational integral for a canonical ensemble of M obstacles in a volume V at a reciprocal temperature β_m. In a quenched grand canonical ensemble of obstacles, the probability of finding M indistinguishable obstacles in this volume is $z_m^M Z_M/(M!\, \Xi_m)$, and the sum over all M gives the mixed pair density

$$\begin{aligned}\rho^{(2)}_{fm}(\mathbf{r}_1,\mathbf{q}_1)&=\rho^{(1)}_{f|m}(\mathbf{r}_1,\mathbf{q}_1)\\&=\Xi_m^{-1}\sum_M\frac{z_m^M Z_M}{M!}\tilde{\rho}^{(1)}_{f|m}(\mathbf{r}_1|\mathbf{q}_1)\\&=\Xi_m^{-1}\sum_M\frac{z_m^M}{(M-1)!}\sum_N\frac{z_f^N}{(N-1)!}\int d\mathbf{q}_2\cdots d\mathbf{q}_M\\&\quad\times[\Xi_f(\mathbf{q}^M)]^{-1}\int d\mathbf{r}_2\cdots d\mathbf{r}_N\\&\quad\times\exp[-\beta U_{NM}(\mathbf{r}^N;\mathbf{q}^M)-\beta_m W_M(\mathbf{q}^M)]\end{aligned}\tag{20}$$

The expansion of Eq. (20) in f-functions generates the initial graphical series for $\rho^{(2)}_{fm}$ and $\rho^{(2)}_{mf}$, which is suitable for the topological reductions outlined earlier. The analysis applied to $\rho^{(2)}_{ff}$ also applies to these functions: the contributing graphs are the subset of those in the equilibrium mixture without shielding sets. The two-body total correlation functions $h_{\alpha\gamma}(\mathbf{x}_1,\mathbf{x}_2)=g_{\alpha\gamma}(\mathbf{x}_1,\mathbf{x}_2)-1$ eliminate the single disconnected graph in $g_{\alpha\gamma}$, and lead to

$h_{\alpha\gamma}(\mathbf{x}_1,\mathbf{x}_2)=$ sum of all topologically distinct, simple, connected graphs with one unity-weighted fluid root point of species α, one unity-weighted fluid root point of species γ, some or no fluid field points representing the function $\rho^{(1)}_f(\mathbf{r})$, some or no obstacle field points representing the function $\rho^{(1)}_m(\mathbf{r})$, some or no f_u bonds between pairs of fluid points, some or no f_v bonds between mixed pairs of points, *and some or no f_w bonds between pairs of obstacle points,* such that the diagrams have no articulation points and no shielding sets (21)

The conditions listed in Eq. (21) (except for the italicized language) will prove common to several additional topological specifications to be made below and, for conciseness, will be designated the *basic specifications.* Note that the restriction on shielding sets eliminates all fluid points and bonds from h_{mm} and correctly reduces this correlation function to that of a pure substance.

As noted above, we imagine the existence of many macroscopic replicas of the system, each of volume V and having a different, but fixed, distribution of obstacles. Under such an assumption, the Helmholtz free energy of the fluid is the average over the ensemble of obstacle realizations, and is expressed by Eq. (4) with $Y(\mathbf{q}^M)=A(\mathbf{q}^M)$, so that $A_f=\langle\hat{A}_f(\mathbf{q}^M)\rangle_M$. Because the entire free energy cannot be written as a sum of graphs in the

f-z representation,[11] the usual analysis[1,2] proceeds through the singlet density. The configurational chemical potential is given by

$$-\beta\mu_f = -\beta\left(\frac{\partial A_{f,t}}{\partial N_t}\right)_{\beta, V_t} = -\beta\left(\frac{\partial(A_{f,t}/V_t)}{\partial(N_t/V_t)}\right)_{\beta, V_t}$$
$$= -\beta\left(\frac{\partial(A_f/V)}{\partial\rho_f}\right)_{\beta, V} = \ln\frac{\rho_f}{z_f} \tag{22}$$

where $A_{f,t}$, V_t, and N_t are the total free energy, volume, and number of particles of the fluid in the entire ensemble of replicas of obstacles. The usual derivation of the free energy requires a term-by-term comparison of the *density* expansions of $\rho_f^{(1)}(\mathbf{r}_1)/z_f^*(\mathbf{r}_1)$ and of $\partial(A_f/V)/\partial\rho_f$. The density expansion of $\rho_f^{(1)}(\mathbf{r}_1)/z_f^*(\mathbf{r}_1)$ can be obtained in the same form as that for $\rho_{ff}^{(2)}(\mathbf{r}_1, \mathbf{r}_2)$, with the minimal set of articulation *field* points also replaced with density field points. The analysis carries through in a straightforward fashion, and the result for the mean configurational Helmholtz free energy is

$-\beta A_f =$ sum of all topologically distinct, connected graphs consisting of one or more fluid $\rho_f^{(1)}$ field points, some or no obstacle $\rho_m^{(1)}$ field points, some or no f_u bonds between pairs of fluid points, some or no f_v bonds between mixed pairs of points, and some or no f_w bonds between pairs of obstacle points, such that the diagrams contain at least two points and are free of articulation field points and of shielding sets (23)

The sum of all graphs with no obstacle points is just the configurational free energy of the pure fluid in the absence of the obstacle field. Subtracting this quantity yields the configurational "free energy of absorption" of the fluid into the matrix

$-\beta\,\Delta A_{\text{abs}} =$ sum of all graphs in Eq. (23) with at least one obstacle point (24)

This quantity differs from the conformational contribution to the constant-volume free energy of mixing of an equilibrium mixture in that is does not include graphs with shielding sets.

Other thermodynamic quantities, such as the internal energy and the presssure, may be expressed as mechanical averages given by Eq. (8). In many instances, the mechanical quantity is a sum of pair contributions

$$X(\mathbf{r}^N; \mathbf{q}^M) = \sum_{i<j} x_{mm}(\mathbf{q}_i, \mathbf{q}_j) + \sum_i \sum_j [x_{mf}(\mathbf{q}_i, \mathbf{r}_j) + x_{fm}(\mathbf{r}_i, \mathbf{q}_j)]$$
$$+ \sum_{i<j} x_{ff}(\mathbf{r}_i, \mathbf{r}_j) \tag{25}$$

It is easy to show that for such a quantity, Eq. (8) leads to the usual mixture expression

$$\begin{aligned}\langle X\rangle =& \frac{1}{2}\int d\mathbf{q}_1\, d\mathbf{q}_2\, x_{mm}(\mathbf{q}_i, \mathbf{q}_j)\, \rho^{(2)}_{mm}(\mathbf{q}_i, \mathbf{q}_j)\\ &+ \frac{1}{2}\int d\mathbf{q}_1\, d\mathbf{r}_1\, [x_{mf}(\mathbf{q}_1, \mathbf{r}_1)\, \rho^{(2)}_{mf}(\mathbf{q}_1, \mathbf{r}_1) + x_{fm}(\mathbf{r}_1, \mathbf{q}_1)\, \rho^{(2)}_{fm}(\mathbf{r}_1, \mathbf{q}_1)]\\ &+ \frac{1}{2}\int d\mathbf{r}_1\, d\mathbf{r}_2\, x_{ff}(\mathbf{r}_1, \mathbf{r}_2)\, \rho^{(2)}_{ff}(\mathbf{r}_1, \mathbf{r}_2) \qquad (26)\end{aligned}$$

The differences between Eqs. (8) and (9) are thus carried entirely by the distribution functions. In some cases, the *m–m* contribution may be absent from Eqs. (25) and (26).

3. ORNSTEIN–ZERNIKE EQUATIONS

Term-by-term evaluation of the diagrams in Eq. (21) is useful only at low densities of both particles and obstacles. In order to develop approximations accurate at higher densities, it is helpful to have an implicit set of equations for the pair correlation functions. In equilibrium mixtures, the Ornstein–Zernike equations have proven a fruitful starting point for the generation of such approximations.(2,13) However, the form of these equations is such that they automatically generate diagrams with shielding sets. To establish suitable Ornstein–Zernike equations for the two-phase random medium, we identify diagrams containing nodal points, i.e., those points that lie on all paths connecting the roots. It is useful to define a direct correlation function $c_{\alpha\gamma}(\mathbf{x}_1, \mathbf{x}_2)$ as

$$c_{\alpha\gamma}(\mathbf{x}_1, \mathbf{x}_2) = \text{sum of all graphs in Eq. (21) with no nodal points} \qquad (27)$$

The structure between nodes or between roots and nodes of the $h_{\alpha\gamma}(\mathbf{x}_1, \mathbf{x}_2)$ in Eq. (21) is thus always that of one of the graphs contributing to one of the $c_{\alpha\gamma}(\mathbf{x}_1, \mathbf{x}_2)$. Thus, $h_{\alpha\gamma}(\mathbf{x}_1, \mathbf{x}_2)$ can be represented as an infinite sum of distinct graphs that are chains of various *c*-bonds. This sum is given explicitly as a sum of successive convolutions of the $c_{\alpha\gamma}(\mathbf{x}_1, \mathbf{x}_2)$ with one another.

In an equilibrium mixture, each of the $h_{\alpha\gamma}(\mathbf{x}_1, \mathbf{x}_2)$ is the sum of *all possible* distinct chains of *c*-bonds that begin at an α-root and end at a γ-root. In the random medium, only those chains with no shielding nodes are present. In order to prevent any two obstacle nodes from forming shielding pairs, the graphs contributing to $h_{ff}(\mathbf{r}_1, \mathbf{r}_2)$ must have *one* uninterrupted sequence of some or no fluid nodes, followed by *one* uninterrupted sequence of some or no obstacle nodes, followed by a final, uninterrupted sequence of some or no fluid nodes. Multiple sequences of obstacle nodes are forbidden. If any obstacle nodes are present, one of the graphs from $c_{fm}(\mathbf{r}_1, \mathbf{q}_1)$ must occur at the beginning of the series of convolutions over obstacle points, followed by one of the graphs from $c_{mf}(\mathbf{q}_1, \mathbf{r}_1)$ at the end of the sequence. Between these may be any number of convolutions over graphs from $c_{mm}(\mathbf{q}_1, \mathbf{q}_2)$ and, on either side, any number of convolutions over diagrams from $c_{ff}(\mathbf{r}_1, \mathbf{r}_2)$. The general structure of these graphs is shown in Fig. 2. The sums over all sequences of chains of c-bonds of the same species are denoted by $C_{mm}(\mathbf{q}_1, \mathbf{q}_2)$ and $C_{ff}(\mathbf{r}_1, \mathbf{r}_2)$, and may be readily evaluated in Fourier space(1,2,12) if both $c_{mm}(\mathbf{q}_1, \mathbf{q}_2)$ and $c_{ff}(\mathbf{r}_1, \mathbf{r}_2)$ are known. In fact, $C_{mm}(\mathbf{q}_1, \mathbf{q}_2)$ is just $h_{mm}(\mathbf{q}_1, \mathbf{q}_2)$.

The average pair distribution function for the fluid can be shown to be given by

$$\begin{aligned}h_{ff}(\mathbf{r}_1, \mathbf{r}_2) = C_{ff}(\mathbf{r}_1, \mathbf{r}_2) + \int d\mathbf{r}_3\, d\mathbf{r}_4\, \rho_f^{(1)}(\mathbf{r}_3)\, \rho_f^{(1)}(\mathbf{r}_4)\, H_{ff}(\mathbf{r}_1, \mathbf{r}_3)\\ \times \Bigg[\int d\mathbf{q}_3\, d\mathbf{q}_4\, \rho_m^{(1)}(\mathbf{q}_3)\, \rho_m^{(1)}(\mathbf{q}_4)\\ \times c_{fm}(\mathbf{r}_3, \mathbf{q}_3)\, H_{mm}(\mathbf{q}_3, \mathbf{q}_4)\, c_{mf}(\mathbf{q}_4, \mathbf{r}_4)\Bigg] H_{ff}(\mathbf{r}_4, \mathbf{r}_2) \qquad (28)\end{aligned}$$

where H_{ff} and H_{mm} are hypervertex functions defined by

$$\begin{aligned}&\rho_\alpha^{(1)}(\mathbf{x}_i)\, \rho_\alpha^{(1)}(\mathbf{x}_j)\, H_{\alpha\alpha}(\mathbf{x}_i, \mathbf{x}_j)\\ &\quad = \rho_\alpha^{(1)}(\mathbf{x}_i)\, \delta(\mathbf{x}_i - \mathbf{x}_j) + \rho_\alpha^{(1)}(\mathbf{x}_i)\, \rho_\alpha^{(1)}(\mathbf{x}_j)\, C_{\alpha\alpha}(\mathbf{x}_i, \mathbf{x}_j)\end{aligned}$$

where $\alpha = (m, f)$ and $\delta(\mathbf{x})$ is a three-dimensional Dirac delta function. While $C_{mm}(\mathbf{q}_i, \mathbf{q}_j)$ is entirely determined by the structure of the medium,

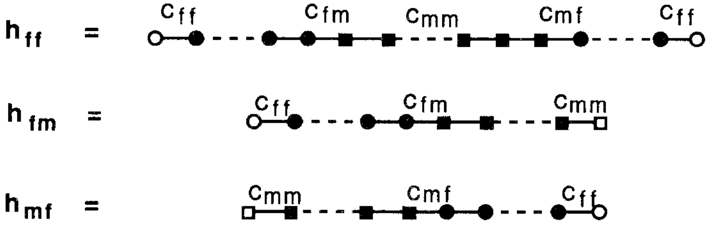

Fig. 2. General structure of the graphs in the total correlation functions $h_{ff}(\mathbf{r}_1, \mathbf{r}_2)$, $h_{fm}(\mathbf{r}_1, \mathbf{q}_1)$, and $h_{mf}(\mathbf{q}_1, \mathbf{r}_1)$. The circles and squares denote fluid and obstacle nodes, respectively. The bonds denote direct correlation functions, as indicated. Only one sequence of obstacle nodes is allowed, in order to avoid the occurrence of shielding sets.

the functions $c_{fm}(\mathbf{r}_i, \mathbf{q}_i)$, $c_{mf}(\mathbf{q}_i, \mathbf{r}_i)$, $C_{ff}(\mathbf{r}_i, \mathbf{r}_j)$, and $h_{ff}(\mathbf{r}_i, \mathbf{r}_j)$ are related only by the single equation (28).

Additional implicit equations may be obtained by examining the nodal structure of the mixed total correlation functions $h_{fm}(\mathbf{r}_1, \mathbf{q}_1)$ and $h_{mf}(\mathbf{q}_1, \mathbf{r}_1)$. In order to prevent the obstacle particle at $\mathbf{q}_1$ and any obstacle node from becoming a shielding pair, the graphs contributing to $h_{fm}(\mathbf{r}_1, \mathbf{q}_1)$ must have *one* uninterrupted sequence of some or no fluid nodes followed by only *one* uninterrupted sequence of some or no obstacle nodes. If obstacle nodes are present, they may arise from any number of convolutions over diagrams from $c_{ff}(\mathbf{r}_1, \mathbf{r}_2)$, followed by one of the diagrams from $c_{fm}(\mathbf{r}_1, \mathbf{q}_1)$ and by any number of convolutions over diagrams from $c_{mm}(\mathbf{q}_1, \mathbf{q}_2)$. The nodal structure of $h_{mf}(\mathbf{q}_1, \mathbf{r}_1)$ is exactly the reverse, with diagrams from $c_{mf}(\mathbf{q}_i, \mathbf{r}_i)$ providing the transition between sequences of like nodes. In terms of the hypervertex functions defined above, $h_{fm}(\mathbf{r}_1, \mathbf{q}_1)$ and $h_{mf}(\mathbf{q}_1, \mathbf{r}_1)$ can be expressed as

$$h_{fm}(\mathbf{r}_1, \mathbf{q}_1) = \int d\mathbf{q}_2\, d\mathbf{r}_2\, \rho_f^{(1)}(\mathbf{r}_2)\, \rho_m^{(1)}(\mathbf{q}_2)\, H_{ff}(\mathbf{r}_1, \mathbf{r}_2) \times c_{fm}(\mathbf{r}_2, \mathbf{q}_2)\, H_{mm}(\mathbf{q}_2, \mathbf{q}_1) \tag{29}$$

and

$$h_{mf}(\mathbf{q}_1, \mathbf{r}_1) = \int d\mathbf{q}_2\, d\mathbf{r}_2\, \rho_m^{(1)}(\mathbf{q}_2)\, \rho_f^{(1)}(\mathbf{r}_2)\, H_{mm}(\mathbf{q}_1, \mathbf{q}_2) \times c_{mf}(\mathbf{q}_2, \mathbf{r}_2)\, H_{ff}(\mathbf{r}_2, \mathbf{r}_1) \tag{30}$$

Equations (28)–(30) are actually the Ornstein–Zernike equations for the random medium. More conventionally, they may be written as

$$h_{mm}(\mathbf{q}_1, \mathbf{q}_2) = c_{mm}(\mathbf{q}_1, \mathbf{q}_2) + \int d\mathbf{q}_3\, c_{mm}(\mathbf{q}_1, \mathbf{q}_3)\, \rho_m^{(1)}(\mathbf{q}_3)\, h_{mm}(\mathbf{q}_3, \mathbf{q}_2) \tag{31}$$

$$h_{mf}(\mathbf{q}_1, \mathbf{r}_1) = c_{mf}(\mathbf{q}_1, \mathbf{r}_1) + \int d\mathbf{q}_3\, c_{mm}(\mathbf{q}_1, \mathbf{q}_3)\, \rho_m^{(1)}(\mathbf{q}_3)\, h_{mf}(\mathbf{q}_3, \mathbf{r}_1) + \int d\mathbf{r}_3\, c_{mf}(\mathbf{q}_1, \mathbf{r}_3)\, \rho_f^{(1)}(\mathbf{r}_3)\, C_{ff}(\mathbf{r}_3, \mathbf{r}_1) \tag{32}$$

$$h_{fm}(\mathbf{r}_1, \mathbf{q}_1) = c_{fm}(\mathbf{r}_1, \mathbf{q}_1) + \int d\mathbf{q}_3\, c_{fm}(\mathbf{r}_1, \mathbf{q}_3)\, \rho_m^{(1)}(\mathbf{q}_3)\, h_{mm}(\mathbf{q}_3, \mathbf{q}_1) + \int d\mathbf{r}_3\, c_{ff}(\mathbf{r}_1, \mathbf{r}_3)\, \rho_f^{(1)} h_{fm}(\mathbf{r}_3, \mathbf{q}_1) \tag{33}$$

$$h_{ff}(\mathbf{r}_1, \mathbf{r}_2) = c_{ff}(\mathbf{r}_1, \mathbf{r}_2) + \int d\mathbf{q}_3\, c_{fm}(\mathbf{r}_1, \mathbf{q}_3)\, \rho_m^{(1)}(\mathbf{q}_3)\, h_{mf}(\mathbf{q}_3, \mathbf{r}_2)$$
$$+ \int d\mathbf{r}_3\, c_{ff}(\mathbf{r}_1, \mathbf{r}_3)\, \rho_f^{(1)}(\mathbf{r}_3)\, h_{ff}(\mathbf{r}_3, \mathbf{r}_1) \tag{34}$$

Iterative substitution among these equations shows that they generate the restricted nodal structures for h_{ff}, h_{mf}, and h_{fm} deduced above.

Equations (31)–(34) differ from those for a true equilibrium mixture in two crucial ways. First, there is no convolution over a fluid field point in the equation for h_{mm}. This should be expected, since Eq. (31) is the true Ornstein–Zernike equation for the obstacle sites alone. It is necessary that this term be absent in order to prevent the introduction of shielding sequences in the other $h_{\alpha\gamma}$. A more subtle difference is the presence of C_{ff} in the second convolution of Eq. (32), which replaces the function h_{ff} in the usual mixture expression. Its introduction prevents the occurrence of shielding pairs of nodal points in all subsequent equations and preserves the symmetry between Eqs. (32) and (33).

It is easy to show that the usual mixture versions of the hypernetted-chain approximation, the Percus–Yevick approximation, and the mean spherical approximation introduce no shielding sets into the direct correlation functions and are therefore readily applied to Eqs. (32)–(34). In generating new or more elaborate approximations, care must be taken to prevent the introduction of shielding sets. These are properly present in an equilibrium mixture, and Percus' functional expansion method$^{(4)}$ for producing higher order versions of these approximations for an equilibrium mixture will eventually generate such improper graphs. Since there is no single partition function for the problem of a fluid in a quenched random medium, the analogous starting point for the Percus analysis is not obvious in this case.

4. FURTHER TOPOLOGICAL REDUCTIONS

The graphical expressions given above for the structure and thermodynamic properties contain the obstacle–obstacle potential explicitly. This potential might not be known, but the pair structure of the obstacles will nearly always be accessible via diffraction methods. Using ideas first introduced by Abe$^{(14)}$ and fully developed by Stell,$^{(3,14)}$ it is possible to identify articulation pairs of obstacle points within the graphs for the obstacle distribution functions. The removal of these pairs gives rise to a residual belonging to the graphical series for h_{mm}. The topological reduction for h_{mf}, h_{fm}, and h_{ff} is straightforward and yields

$h_{\alpha\gamma}(\mathbf{x}_1, \mathbf{x}_2) =$ sum of all graphs consistent with the basic specifications of Eq. (21), some or no h_{mm} bonds connecting pairs of obstacle points, such that there are no articulation pairs of obstacle points (35)

For spherical obstacles, h_{mm} is completely determined by the structure factor of the obstacles. The direct correlation functions $c_{\alpha\gamma}(\mathbf{x}_1, \mathbf{x}_2)$ are given by the sums of all diagrams in (35) with no nodal points.

A further reduction of Eq. (35) may be made by considering the "islands" of obstacle points present in some of the graphs. An island is a set of obstacle points mutually connected via obstacle–obstacle bonds. Islands are *separated* if every path between them contains at least one fluid point. Consider a subset of an island, consisting of either root points or of points directly connected to a fluid point. These n points from an articulation set whose removal disconnects a residual belonging to $h_m^{(n)}(\mathbf{q}^n)$ [i.e., to the sum of *connected* graphs contributing to the n-obstacle distribution function $g_m^{(n)}(\mathbf{q}^n)$]. The $h_m^{(n)}(\mathbf{q}^n)$ may be represented as generalized "bonds" which simultaneously connect n points in a graph and can be used as elements in a further topological reduction,

$h_{\alpha\gamma}(\mathbf{x}_1, \mathbf{x}_2) =$ sum of all graphs consistent with the basic specifications of Eq. (21), with some or no separated $h_m^{(n)}$ bonds connecting sets of obstacle points that are themselves either root points or are directly connected to at least one fluid point by an f_v bond (i.e., there are no articulation obstacle sets of any order) (36)

Note that the $h_m^{(n)}$ functions are represented by graphical series that contain nodal points. When introduced into Eq. (36), they obscure the nodal structure of the parent series and preclude any expression of the $c_{\alpha\gamma}$ in terms of a graphical series with $h_m^{(n)}$ bonds as the only obstacle contributions. However, the full nodal structure of the $h_{\alpha\gamma}$ can be revealed by expanding the $h_m^{(n)}$ functions in terms of $c_m^{(s)}$ functions ($s \leqslant n$), via exhaustive iterative substitution of the nth- and lower-order Ornstein–Zernike equations for the medium into one another. This produces a graphical series whose connective elements include only c_m bonds of various orders. For the pair function h_{mm}, this is the usual chain sum of c_{mm} bonds. For higher order functions, the graphs have branched structures which involve the various pure-obstacle direct correlation functions. Stell$^{(14)}$ has shown that the diagrammatic series for $h_m^{(n)}$ in terms of $c_m^{(s)}$ bonds requires that two c_m bonds have at most a single point in common and that at least two c_m

bonds intersect at every field point. We will refer to such structures as "OZ-consistent." The resulting expression for $c_{\alpha\gamma}$ is then

$c_{\alpha\gamma}(\mathbf{x}_1, \mathbf{x}_2) =$ sum of all graphs consistent with the basic specifications of Eq. (21), with some or no $c_m^{(n)}$ bonds connecting the obstacle points within each separate island in an OZ-consistent fashion, such that there are no nodal points

(37)

Finally we note that, if completely rooted, the set of all obstacle islands in Eq. (36) represents graphs that are products of $h_m^{(n)}$ functions of various orders and contribute to the expression for $g_m^{(s)}$ in terms of $h_m^{(n)}$ functions ($s \geqslant n$). However, not all the required graphs are present, because we have eliminated the articulation circles at fluid points. These structures arise inevitably when the function $g_m^{(s)}$ is expanded in $h_m^{(p)}$ functions ($p \leqslant s$). Returning to the original z–f representation for $\rho_{\alpha\gamma}^{(2)}$, we can once again partition the obstacle points in any one graph into a set that are either root points or directly connected to a fluid point, and a second set that are connected only to other obstacle points. The former subset is used as a reducible set, which leads to a graphical series containing $\rho_m^{(s)}$ functions. These may be replaced with singlet densities and $g_m^{(s)}$ functions. The analysis proceeds just as readily for mixed distribution functions of any order, defined by arguments similar to those that lead to Eq. (20). This produces the topological expression

$\rho_{\alpha,\ldots,\nu}^{(n)}(\mathbf{x}^n) =$ sum of all topologically distinct, simple graphs with root points of the species $\alpha,\ldots,\nu$ $(=m,f)$ representing the functions $z_f^*(\mathbf{r})$ for fluid roots and $\rho_m^{(1)}(\mathbf{q})$ for obstacle roots, at least one fluid root, some or no fluid field points representing $z_f^*(\mathbf{r})$, precisely s obstacle field points ($s \geqslant 0$) representing $\rho_m^{(1)}(\mathbf{q})$ and connected by a single multiobstacle bond representing the function $g_m^{(s)}(\mathbf{q}^s)$, some or no f_u bonds connecting fluid points, such that every obstacle point is either a root or is directly connected to at least one fluid point by an f_v bond, and such that the graphs have no shielding sets

(38)

In order to obtain the preceding representations using standard techniques of topological reduction, it was assumed that the distribution of obstacles was one of quenched equilibrium. However, the expressions appropriate to that particular situation are necessarily embedded in a more general analysis in which the obstacle distribution is decomposed using probability theory alone. The equilibrium expressions relating the various

$g_m^{(n)}$, $h_m^{(n)}$, and $c_m^{(n)}$ do not contain the intermolecular potential, and may be taken as defining equations, applicable even when the structure of the rigid obstacles is far from equilibrium. It is intuitively clear that the most general expression of this problem will involve obstacle distributions of all orders. One is therefore led to suspect that the above expressions involving these higher order functions are indeed general statements for the structure of a mobile phase in equilibrium within a rigid structure of obstacles. In fact, we show elsewhere that an analysis similar to that of Torquato and Stell[6] will generate Eq. (38) directly, without any assumption about the origins of the obstacle distribution. Indeed, that analysis does not require that the obstacle distribution be homogeneous on any length scale. Voids much larger than the obstacles themselves can be accommodated by including distribution functions of appropriately high order. However, the formalism will probably not prove useful unless fluctuations contributing to the obstacle distribution are not *too* different from those observed in typical equilibrium fluids.

5. IDEAL GAS IN A RANDOM MEDIUM

In their analysis of the matrix functions $S^{(n)}(\mathbf{r}^n)$, Torquato and Stell[6] obtain—without recourse to equilibrium statistical mechanics—a Mayer–Montroll expression which is a special case of Eq. (38). Their model requires that the matrix be made up of obstacles impenetrable to the fluid particles (though possibly penetrable to each other), so that there is no ambiguity about the partitioning of the volume into rigid and fluid domains. They note[7] that there is a one-to-one isomorphism between their analysis for the $S^{(n)}(\mathbf{r}^n)$ functions, the probability that n points in a given configuration do not fall within any of the obstacles, and the distribution functions for an ideal gas confined to that same space. This is so because the Torquato–Stell probe functions do not involve any interaction among the probe points. These probe functions $m(\mathbf{r})$ equal unity under exactly the same circumstances for which $f_v = -1$. The explicit Mayer–Montroll expression given by Torquato and Stell generates, for the quantity $S^{(n)}(\mathbf{r}^n)/\prod_i S^{(1)}(\mathbf{r}_i) = g_f^{(n)}(\mathbf{r}^n)$, the same graphical series given by Eq. (38) with $\alpha = \phi = \cdots = v = f$, no fluid field points, no f_u bonds, and all f_v bonds representing a simple hard-core exclusion.

An alternative graphical series for the $S^{(n)}(\mathbf{r}^n)$ is generated from Eq. (35),

$S^{(n)}(\mathbf{q}^n)$ = sum of all topologically distinct, simple graphs with n "probe" root points at positions $\mathbf{r}_1, \ldots, \mathbf{r}_n$, representing the function $S^{(1)}(\mathbf{r}_i)$, some or no obstacle field points representing $\rho_m^{(1)}(\mathbf{q})$,

> some or no separated $h_m^{(n)}$ bonds connecting a set of obstacle points, such that every obstacle point is directly connected to at least one root point by an m bond, and such that the graphs have no articulation points (39)

This formulation differs from that arising from the Mayer–Montroll equations of Torquato and Stell.(7) The latter series contains roots of unit weight and disconnected graphs with articulation points at the roots. The only disconnected graph in Eq. (39) is the one with two roots and no bonds. The function $S^{(1)}(\mathbf{r}_i)$ always reduces to the volume fraction of the matrix (the space not occupied by the obstacles). With the contribution of $S^{(1)}(\mathbf{r}_i)$ made explicit, the series in Eq. (39) may sometimes prove to be easier to manipulate than the original series.

In an approach similar to the one taken here, Torquato and Stell were also able to obtain equivalent expressions for the $S^{(n)}(\mathbf{r}^n)$ via the *equilibrium* hierarchy of Kirkwood and Salzburg. They noted that, when the particles of the mobile phase interact with one another, the Kirkwood–Salzburg hierarchy provides well-defined expressions for $g^{(n)}(\mathbf{r}^n)$ in the two-phase random medium. However, they question how to avoid generating the equilibrium-mixture distribution when the Kirkwood–Salzburg equations for the mixed distributions are considered. From our analysis, it is clear that such coupled, implicit equations must exclude graphs with shielding sets. Because of the highly connected structure of the Kirkwood–Salzburg hierarchy (i.e., because every field point is connected to one root in each term of the equations), this seems not to be a serious problem. If the obstacle distribution functions are fixed *a priori*, then, upon selective iterative substitution to remove higher order fluid functions in favor of f_u and f_v functions, appropriately modified Kirkwood–Slazburg equations will not generate graphs with shielding sets.

The Torquato–Stell (Mayer–Montroll) equations for the case $f_u = 0$ are(7)

$$g_f^{(n)}(\mathbf{r}^n) = \sum_{s=0}^{\infty} \frac{1}{m!} \int d\mathbf{q}^s \, \rho_m^{(s)}(\mathbf{q}^s) \prod_{j=1}^{s} \left\{ \left[\prod_{i=1}^{n} [1 + f_v(\mathbf{r}_i, \mathbf{q}_j)] \right] - 1 \right\} \tag{40}$$

where the definitions $\rho^{(0)} = 0$ and $g^{(0)} = 0$ have been used. The average pair correlation function is

$$\begin{aligned} g_{ff}(\mathbf{r}_1, \mathbf{r}_2) = 1 &+ \rho_m^{(1)} \int d\mathbf{q}_1 \, [f_v(\mathbf{r}_1, \mathbf{q}_1) + f_v(\mathbf{r}_2, \mathbf{q}_1) + f_v(\mathbf{r}_1, \mathbf{q}_1) f_v(\mathbf{r}_2, \mathbf{q}_1)] \\ &+ \frac{[\rho_m^{(1)}]^2}{2!} \int d\mathbf{q}_1 \, d\mathbf{q}_2 \, [f_v(\mathbf{r}_1, \mathbf{q}_1) + f_v(\mathbf{r}_2, \mathbf{q}_1) + f_v(\mathbf{r}_1, \mathbf{q}_1) f_v(\mathbf{r}_2, \mathbf{q}_1)] \\ &\times [f_v(\mathbf{r}_1, \mathbf{q}_2) + f_v(\mathbf{r}_2, \mathbf{q}_2) + f_v(\mathbf{r}_1, \mathbf{q}_2) f_v(\mathbf{r}_2, \mathbf{q}_2)] \\ &\times g_{mm}(\mathbf{q}_1, \mathbf{q}_2) + O(\rho_m^3) \end{aligned} \tag{41}$$

Torquato[16] has discussed a more general class of correlations of which these are a particular case. The functions $S^{(2)}(r)$ and $g_{ff}(r)$ have been computed for a few model media. The calculations are analytic and exact for the case when the matrix consists of randomly placed (i.e., fully penetrable) spheres. This is the random-medium analog of the Widom–Rowlinson penetrable sphere model[17] for equilibrium mixtures. It may also be regarded as the equilibrium problem corresponding to the Lorentz model of kinetic theory,[18,19] with randomly placed scatterers. If a denotes the diameter of the uniformly distributed obstacles,[20]

$$\begin{aligned} g_{ff}(r) &= \exp\left\{\frac{4}{3}\pi\rho a^3\left[1-\frac{3}{4}\frac{r}{a}+\frac{1}{16}\left(\frac{r}{a}\right)^3\right]\right\}, && r<2a \\ &= 1, && r>2a \end{aligned} \tag{42}$$

Torquato and Stell[10] have also considered a medium with the structure corresponding to impenetrable spheres. They showed that, for impenetrable obstacles following *any* distribution, the Mayer–Montroll series (40) is self-truncating, and that the expression for $g_{ff}(r)$ involves only two field points. For obstacles distributed as equilibrium hard spheres, they calculated $g_{ff}(r)$ analytically to second order in the density of the obstacles, and made numerical calculations using the full expression for the obstacle structure.

Several well-established statistical mechanical tools exist for dealing with inhomogeneous fluids. The formalism presented here provides a much needed generalization to the case where the external field responsible for the inhomogeneities is random due to the presence of a disordered array of obstacles. In most cases, the field is statistically homogeneous and isotropic at length scales larger than the dimensions of those obstacles. Such situations occur in a variety of physical problems involving fluids in quenched, disordered matrices. Prominent examples include hydrogen solubility in amorphous metals and alloys, the partitioning and phase behavior of fluids in microporous glasses,[21] and gas solubility in glassy polymers and polymeric membranes. The molecular foundation of important equilibrium processes for the separation of compact macromolecules and colloidal solutes, such as gel permeation chromatography, is directly related to the calculation of the free energy of "absorption" discussed above.

The formalism also lends itself to a series of natural extensions. One of them, which we will discuss in future work, is the study of the percolation of fluid molecules through a quenched, random medium, i.e., of localization–delocalization phenomena. A second, more important one is the microscopic study of molecular fluids[22] and especially of polymeric liquids[23] constrained within random media, through an application of the site–site integral equation treatment due to Chandler and co-workers.

ACKNOWLEDGMENTS

One of us (E.D.G.) is grateful for the support from the U.S. Department of Energy, Office of Basic Energy Sciences.

REFERENCES

1. J.-P. Hansen and I. R. McDonald, *Theory of Simple Liquids* (Academic Press, London, 1976).
2. H. L. Friedman, *A Course in Statistical Mechanics* (Prentice-Hall, Englewood Cliffs, New Jersey, 1985).
3. G. Stell, in *The Equilibrium Theory of Classical Fluids*, H. L. Frisch and J. L. Lebowitz, eds. (Benjamin, New York, 1964), p. II-171.
4. J. K. Percus, in *The Equilibrium Theory of Classical Fluids*, H. L. Frisch and J. L. Lebowitz, eds. (Benjamin, New York, 1964), p. II-33.
5. H. L. Frisch, *Trans. Rheol. Soc.* **9**:293 (1965).
6. S. Torquato and G. Stell, *J. Chem. Phys.* **77**:2071 (1983).
7. S. Torquato and G. Stell, *J. Chem. Phys.* **78**:3262 (1983).
8. S. Torquato and G. Stell, *J. Chem. Phys.* **79**:1505 (1983).
9. S. Torquato and G. Stell, *J. Chem. Phys.* **80**:878 (1984); **81**:980 (1985).
10. G. Stell, in *Studies in Statistical Mechanics*, Vol. 12, J. L. Lebowitz, ed. (North-Holland, Amsterdam, 1985).
11. T. Morita and K. Hiroike, *Prog. Theor. Phys.* **25**:537 (1961).
12. H. C. Andersen, in *Statistical Mechanics, Part A*, B. J. Berne, ed. (Plenum, New York, 1977).
13. L. S. Ornstein and F. Zernike, *Proc. Acad. Sci. (Amsterdam)* **17**:793 (1914).
14. G. Stell, in *Phase Transitions and Critical Phenomena*, Vol. 5B, C. Domb and M. S. Green, eds. (Academic Press, London, 1975).
15. J. E. Mayer and E. Montroll, *J. Chem. Phys.* **9**:2 (1941).
16. S. Torquato, *J. Stat. Phys.* **45**:843 (1986).
17. B. Widom and J. S. Rowlinson, *J. Chem. Phys.* **52**:1670 (1970).
18. E. H. Hauge, in *Transport Phenomena*, G. Kirczenow and J. Marro, eds. (Springer, Berlin, 1974).
19. M. H. Ernst, in *Recent Developments in Nonequilibrium Thermodynamics*, J. Casas-Vázquez, D. Jou, and J. M. Rubí, eds. (Springer, Berlin, 1986).
20. H. L. Weissberg, *J. Appl. Phys.* **34**:2636 (1963).
21. M. C. Goh, W. I. Goldburg, and C. M. Knobler, *Phys. Rev. Lett.* **58**:1008 (1987).
22. D. Chandler and H. C. Andersen, *J. Chem. Phys.* **57**:1930 (1972).
23. J. G. Curro and K. S. Schweizer, *Macromolecules* **20**:1928 (1987).